Showcasing research from Professor Shionoya's laboratory, Department of Chemistry, Graduate School of Science, the University of Tokyo, Tokyo, Japan.

Synthesis and molecular structural studies of racemic chiral-at-vanadium(v) complexes using an unsymmetric achiral phenolic bidentate ligand

Chiral-at-metal complexes with chirality only at the metal centre due to the asymmetric arrangement of the achiral ligands have been widely used as asymmetric catalysts and chiroptical materials, and new possibilities of chiral metal complexes have attracted much attention. In this study, we have synthesised racemic mononuclear oxovanadium(v) complexes [V(O)X**L** (**1**: X = O*t*-Bu, **2**: X = Cl)] [H_2**L**: 2,2′-methylene bis(4,6-di-*tert*-butylphenol)(4′-*tert*-butyl-6′-(1-adamantyl)phenol)] using an achiral and unsymmetric phenolic bidentate ligand (H_2**L**) by experiments and theoretical calculations. This study will provide a new design strategy for tetrahedral *chiral-only-at-vanadium* complexes.

As featured in:

See Mitsuhiko Shionoya *et al.*, *Dalton Trans.*, 2023, **52**, 3295.

ROYAL SOCIETY OF CHEMISTRY

rsc.li/dalton

Registered charity number: 207890

Dalton Transactions

ROYAL SOCIETY OF CHEMISTRY

PAPER

View Article Online
View Journal | View Issue

Cite this: *Dalton Trans.*, 2023, **52**, 3295

Synthesis and molecular structural studies of racemic chiral-at-vanadium(v) complexes using an unsymmetric achiral phenolic bidentate ligand†

Koichi Nagata,‡[a] Ayako Hino,[a] Hitoshi Ube,[a] Hiroyasu Sato[b] and Mitsuhiko Shionoya *[a]

Received 23rd October 2022,
Accepted 4th January 2023

DOI: 10.1039/d2dt03436k

rsc.li/dalton

Mononuclear oxovanadium(v) complexes [V(O)X**L** (**1**: X = O*t*-Bu, **2**: X = Cl)] [H_2**L**: 2,2′-methylene bis(4,6-di-*tert*-butylphenol)(4′-*tert*-butyl-6′-(1-adamantyl)phenol)] directed towards asymmetric catalysis have been synthesised as racemic compounds using an unsymmetric and achiral phenolic bidentate ligand (H_2**L**), and NMR and UV-vis absorption spectroscopies, single-crystal X-ray diffraction, and IR spectroscopy revealed their racemic *chiral-at-vanadium* structures in solution and in the crystal. In addition, theoretical calculations revealed that the HOMO–LUMO energy gap is smaller for unsymmetric ligands, which promotes d-orbital splitting of the metal centre.

Introduction

Chiral-at-metal complexes, which have chirality only at the metal centre due to the asymmetric arrangement of the achiral ligands, have attracted much attention in recent years and are widely used for asymmetric catalysis and chiroptical properties.[1,2] However, most of them are related to relatively inert octahedral metal complexes, and the control of metal centre chirality of tetrahedral metal complexes has remained an open question due to their lability and rapid racemisation.[3] Recently, we have reported the successful asymmetric construction of a tetrahedral chiral-at-zinc complex with high configuration stability using a designed unsymmetric tridentate ligand, opening up new possibilities for tetrahedral chiral-at-metal complexes that can be used as asymmetric catalysts.[4]

Vanadium is known as an important element in catalytic reactions as well as bioactive systems, and there has been much research on ligand design to improve the catalytic reactivity of oxovanadium complexes in particular.[5–11] Recently, enantiomeric excess (ee) measurements of chiral compounds have been reported using the absorption properties of oxovanadium complexes with aminotriphenolate-type tetradentate ligands, which are expected to serve as molecular sensors specific to their coordination structures.[12]

Vanadium(v) complexes can form a variety of coordination structures. For example, $V(O)(OMe)_3$ forms an oligomeric structure in the crystal, and the vanadium centre adopts an octahedral structure.[13] On the other hand, when bulky alkoxides or phenoxides are used as ligands, the complex exists as a monomer and the vanadium centre exhibits a tetrahedral structure.[14–17] In general, vanadium complexes are reported to be more stable in a higher-coordinated structure than in a four-coordinate structure.[18] This is because the early-transition-metal, vanadium(v), is electron-deficient, and the alkoxy bridges the central metal to the electron-rich structure. Vanadium complexes with a variety of coordination structures have been synthesised and their reactivity and optical properties have been investigated, but most of them are penta- or hexacoordinate vanadium complexes.[19] Here we report the synthesis and structural characterisation of mononuclear oxovanadium(v) complexes (**1** and **2**) with a tetrahedral structure using an unsymmetric bidentate ligand with bulky substituents to introduce chirality to the metal centre, and the stability and electronic properties of these racemic *chiral-at-vanadium* complexes in solution and in the solid state. Furthermore, the d-orbital splitting of the metal centre coordinated by the unsymmetric achiral ligand was promoted, and so its effect on their electronic properties was revealed by its NMR and UV-vis absorption spectroscopies, single-crystal X-ray diffraction, IR spectroscopy and DFT calculations.

[a]*Department of Chemistry, Graduate School of Science, The University of Tokyo, 7-3-1 Hongo, Bunkyo-ku, Tokyo 113-0033, Japan. E-mail: shionoya@chem.s.u-tokyo.ac.jp*
[b]*Rigaku Corporation, 3-9-12 Matsubara-cho, Akishima, Tokyo 196-8666, Japan*

†Electronic supplementary information (ESI) available: Experimental details, characterisation, single X-ray diffraction data, selected spectra and theoretical calculation details. Cartesian coordinates for the calculated structures (xyz file). CCDC 2210585 and 2210598. For ESI and crystallographic data in CIF or other electronic format see DOI: https://doi.org/10.1039/d2dt03436k

‡Present Address: Department of Chemistry, Graduate School of Science, Tohoku University, Sendai 980-8578, Japan.

Results & discussion

Characterisation of oxovanadium(v) complexes 1 and 2

The reaction of $V(O)X_3$ (X = O*t*-Bu, Cl) with the unsymmetrical achiral bidentate ligand H_2**L** in $CHCl_3$ at room temperature gave monomeric tetrahedral oxovanadium(v) complexes rapidly and quantitatively (Scheme 1). The ^{1}H NMR spectra of oxovanadium(v) complexes **1** and **2** showed diastereotopic methylene proton signals split into doublets [**1**: 4.40, 3.60 ppm (J = 13.7 Hz); **2**: 4.74, 3.72 ppm (J = 14.6 Hz)]. The ^{51}V NMR spectrum of complex **1** showed a singlet at δ = −498.1 ppm ($w_{1/2} \approx 198$ Hz), which is comparable to the reported chemical shift values of the tetrahedral complexes.[19,20] In addition, **2** showed a singlet at δ = −244.3 ppm ($w_{1/2} \approx 347$ Hz), which was shifted further downfield than that of **1**. The different chemical shifts of the signals of **1** and **2** are due to the different electron-withdrawing or electron-donating strengths of the coordinating chlorine atom or alkoxide and phenoxide, respectively. The solid-state ATR-IR spectra of **1** and **2** showed signals assigned to their V=O stretching vibrations at 1002 (ν_{calcd} = 1101 cm^{-1}) and 1007 cm^{-1} (ν_{calcd} = 1116 cm^{-1}), respectively.

The tetrahedral structures of oxovanadium(v) complexes **1** and **2** were determined by X-ray crystallographic analyses (Fig. 1), and the geometries of their V(1) centres are τ_4 = 0.98 and 0.96 for **1** and **2**, respectively,[21] with the internal coordination sphere angles from 107.12(5)° to 111.80(5)°. Both **1** and **2** have a monomeric structure and no intermolecular contacts within *ca.* 2.7 Å. Their V(1)=O(1) bond distances [**1**: 1.5862(10) Å, **2**: 1.581(10) Å] are almost the same as those of the reported tetrahedral complexes (*ca.* 1.58 Å).[14,15,19,20,22] The V–O single bonds for **1** [V(1)–O(2) 1.7902(10) and V(1)–O(3) 1.7892(10)] are slightly longer than those of **2** [V(1)–O(2) 1.771(10) and V(1)–O(3) 1.744(9)]. This difference between structures of **1** and **2** can be attributed to the strong electron-withdrawing nature of the chlorine ligand of **2**, which shortens the V–O bond lengths of the coordinated oxygen atoms due to the strong donating natures of the oxygen atoms attached to the vanadium(v) centre. The eight-membered chelate ring of **2** adopts a boat–boat conformation (Fig. 1d), as does the reported complex [V(O)(ultra)Cl; ultra = 2,2′-CH_2(4-Me,6-*t*-Bu$C_6H_2O^-$)$_2$],[22] while **1** adopts a boat–chair conformation (Fig. 1b).

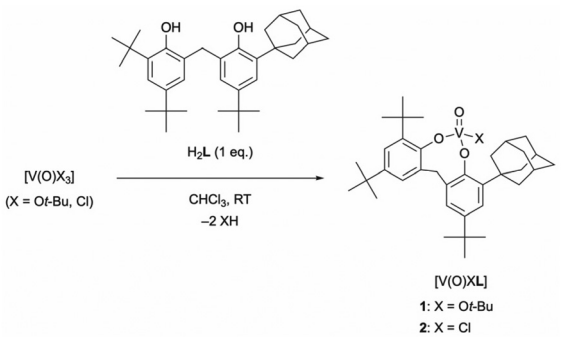

Scheme 1 Synthesis of tetrahedral oxovanadium(v) complexes (**1** and **2**).

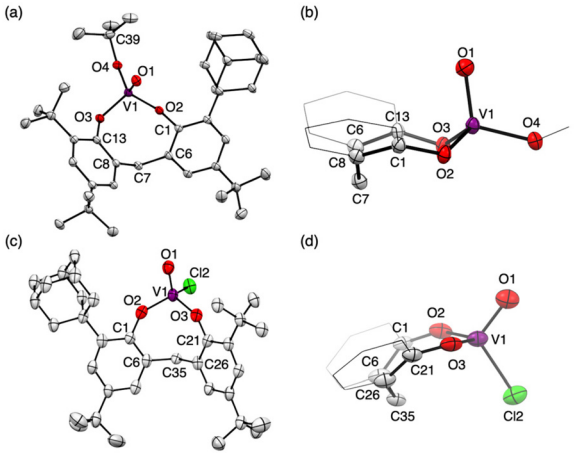

Fig. 1 Molecular structures of **1** (a) and **2** (c). Side views of the eight-membered chelate ring (b: **1**, d: **2**). Thermal displacement ellipsoids are set at the 50% probability level; hydrogen atoms have been omitted for clarity. Two crystallographically independent molecules of **2** were found in the unit cell. Only one of them is shown here (for details, see Fig. S35 and S36 in the ESI†).

DFT calculations

To obtain further information with respect to their geometry, density functional theory (DFT) calculations at the B3LYP[23]/Def2SVP[24] theoretical level were performed for the complete molecular structures of oxovanadium(v) complexes **1** and **2**. The molecular structures of **1** and **2** in the crystalline state were reproduced in the DFT calculations, as can be seen by comparing the selected bond lengths and angles of the crystal structures with the optimised geometries of **I** and **IV** (Table 1). Among the structures calculated for the oxovanadium complexes [V(O)X**L**], boat–boat conformations **I** and **II**

Table 1 Structures of the four minima on the calculated single potential energy surface of V(O)X**L**

	boat–boat		boat–chair	
● = C or CH_2	**I**	**II**	**III**	**IV**
X = O*t*-Bu				
θ [°]	147.2	143.6	130.1	131.7 [127.67(5)][c]
	142.6	137.2	129.3	134.8 [129.91(5)][c]
d [Å]	3.22	3.26	3.37	3.45 [3.419(5)][c]
$\Delta G^{a,b}$	0.00	+1.95	+6.46	+2.12
X = Cl				
θ [°]	149.8 [147.0(3)][c]	145.7	145.7	135.8
	148.0 [142.2(3)][c]	136.0	136.1	131.1
d [Å]	3.29 [3.216(3)][c]	3.27	3.27	3.47
$\Delta G^{a,b}$	0.00	+2.70	+2.78	+2.31

[a] Calculated at the B3LYP/Def2SVP theoretical level. [b] At 298.15 K, in kcal mol^{-1}. [c] XRD results. Substituents of the bidentate ligand have been omitted for clarity.

and boat–chair conformations **III** and **IV** were found as the energy equilibrium structures on the potential energy hypersurface in the ground state. For the hydrocarbon cyclooctane, the boat–chair conformation is more stable than the boat–boat structure due to steric hindrance.[25–27] Furthermore, the bulky substituents tend to be located in the equatorial positions. In contrast, for the oxovanadium complexes, the DFT calculations suggest that form **I** is the most stable structure in the cases of **1** and **2**. The distance (d) between the vanadium and carbon atoms of the CH_2 moiety in the boat–boat structure (**I**) is shorter than the sum of their van der Waals radii (3.75 Å),[28] suggesting electronic interactions between them. Even if an equilibrium exists among these structures, the low equilibrium constant suggests that structure **I** is predominant in solution.

To evaluate the stabilizing effect of the boat–boat structure **I**, NBO calculations[29] for **I–IV** were performed at the B3LYP/Def2SVP theoretical level. In the NBO calculations, the NBO 7.0 program was used to estimate the second-order perturbation of **I–IV** based on the donation of the lone pairs of O/Cl atoms to π*(V═O) orbitals or vacant 3d(V) orbitals. These interaction energies were highest for the boat–boat structure **I**, where the V═O site is equatorial (for the details; see Fig. S31 and Table S5 in ESI†). Furthermore, interactions between the π (C–H) and vacant π*(V═O) orbitals of the bridged CH_2 moiety were observed only in the boat–boat structure **I**, with the interaction energies estimated to be 1.87 (X = O*t*-Bu) and 1.41 kcal mol^{-1} (X = Cl), respectively. These results mean that oxovanadium(v) complexes **1** and **2** are most similar to structure **I** in solution and are also consistent with their UV-vis spectra. The HOMO and LUMO orbitals of **1** and **2** represent the π orbitals on the aromatic rings of the bidentate ligand and the vacant 3d(V) orbitals, respectively (Fig. 2).

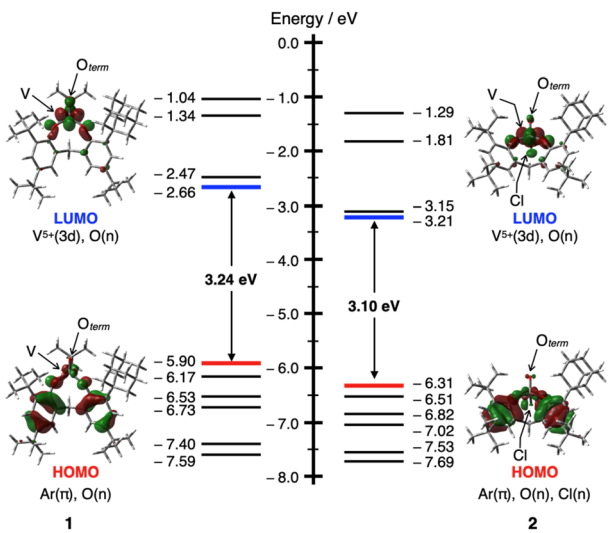

Fig. 2 An energy diagram showing the frontier Kohn–Sham orbitals and energy values for **1** (left) and **2** (right) calculated at the B3LYP/Def2SVP theoretical level (isosurface level: 0.04 e au^{-3}).

UV-vis absorption spectra

The UV-vis absorption spectra of oxovanadium(v) complexes **1** and **2** provided further insight into their structure in solution. In $CHCl_3$, **1** showed a broad absorption band with a maximum at 419 nm (ε = 6600). Time-dependent density functional theory (TD-DFT) calculations of **1** suggested that a broad absorption band with a maximum at 419 nm was considered to be a ligand-to-metal charge-transfer (LMCT) [π (bisphenolate ligand) → V(3d)] transition, and that the minimum energy absorption band at 330 nm (ε = 6900) was considered to be an intraligand charge transfer (ILCT) [π → π* (bisphenolate ligand)] transition (see Tables S1, S2 and Fig. S29 in the ESI†).

The UV-vis spectrum of **2** in $CHCl_3$ also showed characteristic absorption maxima at 472 nm (ε = 8800) and 592 nm (shoulder, ε = 4200), consistent with LMCT [π (bisphenolate ligand) → V(3d)] (see Tables S3, S4 and Fig. S30 in ESI†). The maximum absorption wavelength of **2** was red-shifted compared to that of **1**, possibly due to the chlorine substituent effect, which lowers the LUMO [V(3d)] and reduces the HOMO–LUMO gap (Fig. 3).

To discuss the effect of the unsymmetric bidentate ligand, we synthesised an oxovanadium(v) complex [V(O)(O*t*-Bu)**L**′] (**3**) with a symmetrical bidentate ligand 2,2′-methylenebis[4,6-di-*tert*-butylphenol] (H_2**L**′). The absorption coefficient of **1** was larger than that of **3** (see Fig. S28 in the ESI†), suggesting that the use of an unsymmetric ligand promotes d-orbital splitting of the metal centre of **1**. DFT calculations also suggested that the LUMO energy level of **1** (−2.66 eV) was slightly lower than that of **3** (−2.46 eV), but that of the HOMO is similar (−5.90 eV for **1** and −5.91 eV for **3**). Thus, the HOMO–LUMO energy gap is smaller for **1** (3.24 eV) than for **3** (3.45 eV) (Fig. S32†).

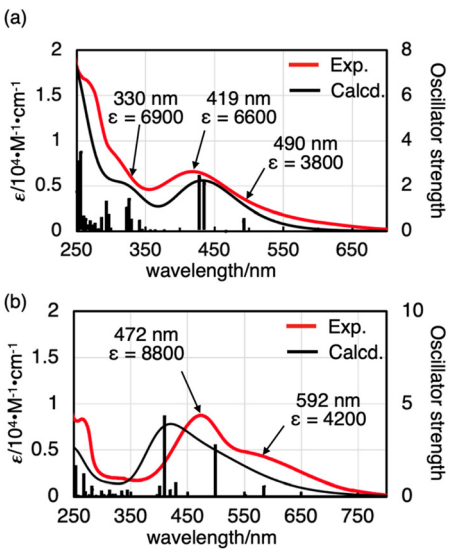

Fig. 3 UV-vis absorption spectra (red lines) of (a) **1** (1.1 × 10^{-3} M) and (b) **2** (4.0 × 10^{-5} M) in $CHCl_3$ (293 K), along with the computed spectrum of V(O)XL (black lines) at the B3LYP/Def2SVP (PCM: $CHCl_3$) theoretical level.

Conclusion

The synthesis, structure and photophysical properties of the racemic tetrahedral oxovanadium(v) complexes **1** and **2** with chirality at the metal centre are described above. These complexes are thermally stable solids, and their molecular structures have been clearly assigned on the basis of spectroscopic and crystallographic analyses and theoretical calculations. Since the structure of the V(O)X**L** synthesised in this study is chiral, the conversion of racemic compounds to diastereomeric complexes by ligand exchange with chiral alcohols is being investigated for the asymmetric induction of the metal-centered chirality.

Experimental

Materials and methods

All the manipulations were performed under a nitrogen atmosphere, either by the Schlenk technique or in a glove box. All solvents were purified by standard methods, and trace amounts of oxygen and water remaining in the solvents were thoroughly removed by the freeze–pump–thaw method and activated MS4A, respectively. ^{1}H, ^{13}C, ^{51}V and 2D NMR spectra were measured on a Bruker AVANCE III-500 (500 MHz) spectrometer. Tetramethylsilane was used as the internal standard for ^{1}H NMR measurements when chloroform-*d* was used as the solvent. When chloroform-*d* (δ 77.16 ppm) was used as the solvent, the residual solvent signal was used to calibrate the ^{13}C NMR measurements. ^{51}V (132 MHz) NMR spectra were recorded on a Bruker AVANCE III-500 spectrometer using V(O)Cl_3 in chloroform-*d* (δ 0 ppm) as an external standard. ESI-TOF mass data were recorded on a Micromass LCT Premier XE mass spectrometer. Unless otherwise noted, experimental conditions were as follows (ion mode, positive; capillary voltage, 3000 V; sample cone voltage, 30 V; desolvation temperature, 150 °C; source temperature, 80 °C). UV-vis absorption spectra in $CHCl_3$ were recorded on a JASCO V-770 UV-vis spectrophotometer. IR spectra were recorded on a Jasco FT/IR 4200 with an ATR equipment. Elemental analysis was performed at the Microanalytical Laboratory of the University of Tokyo. 6,6′-Methylenebis(2,4-di-*tert*-butylphenol),[30] 2,4-di-*tert*-butyl-6-(5-*tert*-butyl-2-hydroxybenzyl)-methylphenol[30] and oxovanadium (v) tri-*tert*-butoxide [V(O)(O*t*-Bu)$_3$][31] were prepared according to a literature.

Synthetic procedures

Synthesis of *rac*-V(O)(O*t*-Bu)L (1): complexation of H_2L with V(O)(O*t*-Bu)$_3$. V(O)(O*t*-Bu)$_3$ (14.0 mg, 48.9 μmol, 1.0 eq.) and H_2**L** (24.6 mg, 48.9 μmol, 1.0 eq.) were mixed in 2.5 mL of $CHCl_3$ and the resultant solution was stirred at room temperature for 10 min. The solvent and *t*-BuOH generated was then removed by evaporation, 2.5 mL of $CHCl_3$ was added again and the solution was stirred at room temperature for 15 h. The solution was filtered through a glass fibre filter paper and the solvent was removed by evaporation to afford **1** as a brown solid (30.0 mg, 46.8 μmol, 96% yield). ^{1}H NMR (500 MHz, $CDCl_3$): δ 7.37 (m, 3H), 7.23 (s, 1H), 7.19 (s, 1H), 4.51 (d, J = 13.7 Hz, 1H), 3.41 (d, J = 13.7 Hz, 1H), 2.10 (m, 9H), 1.78 (s, 6H), 1.71 (s, 9H), 1.42 (s, 9H), 1.32 (s, 18H); ^{51}V NMR (132 MHz, $CDCl_3$): δ −498.1 (broad, $w_{1/2}$ 198 Hz); ^{13}C{^{1}H} NMR (126 MHz, $CDCl_3$): δ 162.6 (C, *ipso*-Ar), 162.4 (C, *ipso*-Ar), 146.3 (C, *p*-Ar), 146.1 (C, *p*-Ar), 136.5 (C, *o*-Ar), 136.5 (C, *o*-Ar), 128.3 (C, *o*-Ar), 128.3 (C, *o*-Ar), 125.4 (C, *o*-Ar), 125.1 (CH, *m*-ArH), 122.9 (CH, *m*-ArH), 122.7 (CH, *m*-ArH), 41.8 (CH_2, Ad), 38.0 (C, 1-Ad), 37.2 (CH_2, Ad), 35.7 (C, *o*-Ar(*t*-Bu)), 34.74 (CH_2, benzyl), 34.68 (C, *p*-Ar(*t*-Bu)), 31.7 (C, *p*-Ar(*t*-Bu)), 31.7 (C, *p*-Ar(*t*-Bu)), 30.9 (2C, CH_3, *p*-Ar(*t*-Bu)), 29.3 (CH_3, *o*-Ar(*t*-Bu)).

Synthesis of *rac*-V(O)ClL (2): complexation of H_2L with V(O)Cl_3. V(O)Cl_3 (10.0 μL, 0.106 mmol, 1.0 eq.) and H_2**L** (53.8 mg, 0.107 mmol, 1.0 eq.) were mixed in 5 mL of $CHCl_3$ and the resultant solution was stirred at room temperature for 10 min. The solvent and HCl generated was then removed by evaporation, 5 mL of $CHCl_3$ was added again and the solution was stirred at room temperature for 15 h. The solution was filtered through a glass fibre filter paper and the solvent was removed by evaporation to afford **2** as a dark purple solid (57.9 mg, 0.096 mmol, 90% yield). ^{1}H NMR (500 MHz, $CDCl_3$): δ 7.37 (m, 2H), 7.23 (d, J = 2.2 Hz, 1H), 7.17 (d, J = 2.2 Hz, 1H), 4.74 (d, J = 14.6 Hz, 1H), 3.72 (d, J = 14.6 Hz, 1H), 2.13 (m, 9H), 1.82 (q, J = 12.0 Hz, 6H), 1.46 (s, 9H), 1.32 (s, 9H), 1.31 (s, 9H); ^{51}V NMR (132 MHz, $CDCl_3$): δ −244.3 (broad, $w_{1/2} \approx$ 347 Hz); ^{13}C{^{1}H} NMR (126 MHz, $CDCl_3$): δ 171.8 (C, *ipso*-Ar), 171.1(C, *ipso*-Ar), 150.0(C, *p*-Ar), 149.6(C, *p*-Ar), 141.4(C, *o*-Ar), 141.0(C, *o*-Ar), 138.3(C, *o*-Ar), 137.6(C, *o*-Ar), 125.3 (CH, *m*-ArH), 125.0 (CH, *m*-ArH), 122.2 (CH, *m*-ArH), 122.2 (CH, *m*-ArH), 41.7 (CH_2, Ad), 38.2 (C, 1-Ad), 37.1 (CH_2, Ad), 35.9 (C, *o*-Ar(*t*-Bu)), 35.5 (CH_2, benzyl), 35.1 (C, *p*-Ar(*t*-Bu)), 35.1 (C, *p*-Ar(*t*-Bu)), 31.5 (2C, CH_3, *p*-Ar(*t*-Bu)), 30.6 (CH_3, *o*-Ar(*t*-Bu)), 29.2 (CH, Ad); elemental analysis (calcd for $C_{35}H_{48}ClO_3V$ (V(O)Cl**L**), found): C (69.70, 70.57) H (8.02, 8.01).

Author contributions

K.N. conceived the development of oxovanadium(v) complexes and performed DFT calculations. A.H. performed the experiments and characterization. K.N. drafted the manuscript. M.S. directed the project and completed the manuscript. H.S. performed the X-ray crystallographic measurements and structure determination. All authors contributed to the analysis and interpretation of the data and commented on the final draft of the manuscript.

Conflicts of interest

There are no conflicts to declare.

Acknowledgements

This work was supported by JSPS KAKENHI Grant Number JP21H05022 (M. S.) and JP18K14236 (K. N.), MEXT KAKENHI

Grant Number JP16H06509 (M. S.) and a Sasagawa Scientific Research Grant from the Japan Science Society (K. N.). A. H. acknowledges Materials Education program for the future leaders in Research, Industry, and Technology (MERIT). Calculations for complexes **1** and **2** were performed using the Research Centre for Computational Science, Okazaki, Japan (Project: 20-IMS-C100).

References

1 E. B. Bauer, *Chem. Soc. Rev.*, 2012, **41**, 3153–3167.
2 H. Huo, X. Shen, C. Wang, L. Zhang, P. Röse, L.-A. Chen, K. Harms, M. Marsch, G. Hilt and E. Meggers, *Nature*, 2014, **515**, 100.
3 V. Desvergnes-Breuil, V. Hebbe, C. Dietrich-Buchecker, J. P. Sauvage and J. Lacour, *Inorg. Chem.*, 2003, **42**, 255–257.
4 K. Endo, Y. Liu, H. Ube, K. Nagata and M. Shionoya, *Nat. Commun.*, 2020, **11**, 6263.
5 E. Amadio, J. González-Fabra, D. Carraro, W. Denis, B. Gjoka, C. Zonta, K. Bartik, F. Cavani, S. Solmi, C. Bo and G. Licini, *Adv. Synth. Catal.*, 2018, **360**, 3286–3296.
6 J. A. L. da Silva, J. J. R. F. da Silva and A. J. L. Pombeiro, *Coord. Chem. Rev.*, 2011, **255**, 2232–2248.
7 R. R. Langeslay, D. M. Kaphan, C. L. Marshall, P. C. Stair, A. P. Sattelberger and M. Delferro, *Chem. Rev.*, 2019, **119**, 2128–2191.
8 C. Bolm, *Coord. Chem. Rev.*, 2003, **237**, 245–256.
9 S. Takizawa, H. Gröger and H. Sasai, *Chem. – Eur. J.*, 2015, **21**, 8992–8997.
10 H. Pellissier, *Coord. Chem. Rev.*, 2015, **284**, 93–110.
11 H. Pellissier, *Coord. Chem. Rev.*, 2020, **418**, 213385.
12 P. Zardi, K. Wurst, G. Licini and C. Zonta, *J. Am. Chem. Soc.*, 2017, **139**, 15616–15619.
13 H. M. S. Charles, N. Caughlan and K. Watenpaugh, *Inorg. Chem.*, 1966, **5**, 2131–2134.
14 F. J. Feher and J. F. Walzer, *Inorg. Chem.*, 1991, **30**, 1689–1694.
15 J. Spandl, I. Brüdgam and H. Hartl, *Z. Anorg. Allg. Chem.*, 2000, **626**, 2125–2132.
16 D. C. Crans, H. J. Chen and R. A. Felty, *J. Am. Chem. Soc.*, 1992, **114**, 4543–4550.
17 D. L. H. Richard, A. Henderson, Z. Janas, R. L. Richards, P. Sobota and S. Szafert, *J. Organomet. Chem.*, 1998, **554**, 195–201.
18 J. Y. Kempf, B. Maigret and D. C. Crans, *Inorg. Chem.*, 1996, **35**, 6485–6494.
19 C. Redshaw, M. J. Walton, M. R. J. Elsegood, T. J. Prior and K. Michiue, *RSC Adv.*, 2015, **5**, 89783–89796.
20 F. Ge, Y. Dan, Y. Al-Khafaji, T. J. Prior, L. Jiang, M. R. J. Elsegood and C. Redshaw, *RSC Adv.*, 2016, **6**, 4792–4802.
21 L. Yang, D. R. Powell and R. P. Houser, *Dalton Trans.*, 2007, 955–964.
22 P. J. Toscano, E. J. Schermerhorn, C. Dettelbacher, D. Macherone and J. Zubieta, *J. Chem. Soc., Chem. Commun.*, 1991, 933–934.
23 S. Grimme, *J. Chem. Phys.*, 2006, **124**, 034108.
24 F. Weigend and R. Ahlrichs, *Phys. Chem. Chem. Phys.*, 2005, **7**, 3297–3305.
25 J. B. Hendrickson, *J. Am. Chem. Soc.*, 1967, **89**, 7036–7043.
26 K. B. Wiberg, *J. Org. Chem.*, 2003, **68**, 9322–9329.
27 P. Khalili, C. B. Barnett and K. J. Naidoo, *J. Chem. Phys.*, 2013, **138**, 184110.
28 S. S. Batsanov, *Inorg. Mater.*, 2001, **37**, 871–885.
29 E. D. Glendening, C. R. Landis and F. Weinhold, *J. Comput. Chem.*, 2019, **40**, 2234–2241.
30 G. Sartori, F. Bigi, R. Maggi and C. Porta, *Tetrahedron Lett.*, 1994, **35**, 7073–7076.
31 C. Redshaw, M.-J. Walton, D.-S. Lee, C. Jiang, M.-R. J. Elsegood and K. Michiue, *Chem. – Eur. J.*, 2015, **21**, 5199–5210.